

The Effect of Atmospheric Water Vapor on Neutron Count in the Cosmic-Ray Soil Moisture Observing System

R. ROSOLEM*

Department of Hydrology and Water Resources, University of Arizona, Tucson, Arizona

W. J. SHUTTLEWORTH

Department of Hydrology and Water Resources, and Department of Atmospheric Sciences, University of Arizona, Tucson, Arizona

M. ZREDA AND T. E. FRANZ

Department of Hydrology and Water Resources, University of Arizona, Tucson, Arizona

X. ZENG

Department of Atmospheric Sciences, University of Arizona, Tucson, Arizona

S. A. KURC

School of Natural Resources and Environment, University of Arizona, Tucson, Arizona

(Manuscript received 15 August 2012, in final form 15 April 2013)

ABSTRACT

The cosmic-ray method for measuring soil moisture, used in the Cosmic-Ray Soil Moisture Observing System (COSMOS), relies on the exceptional ability of hydrogen to moderate fast neutrons. Sources of hydrogen near the ground, other than soil moisture, affect the neutron measurement and therefore must be quantified. This study investigates the effect of atmospheric water vapor on the cosmic-ray probe signal and evaluates the fast neutron response in realistic atmospheric conditions using the neutron transport code Monte Carlo N-Particle eXtended (MCNPX). The vertical height of influence of the sensor in the atmosphere varies between 412 and 265 m in dry and wet atmospheres, respectively. Model results show that atmospheric water vapor near the surface affects the neutron intensity signal by up to 12%, corresponding to soil moisture differences on the order of $0.10 \text{ m}^3 \text{ m}^{-3}$. A simple correction is defined to identify the true signal associated with integrated soil moisture that rescales the measured neutron intensity to that which would have been observed in the atmospheric conditions prevailing on the day of sensor calibration. Use of this approach is investigated with in situ observations at two sites characterized by strong seasonality in water vapor where standard meteorological measurements are readily available.

1. Introduction

The accuracy with which soil moisture is predicted by numerical models is of importance for weather and seasonal climate projections (Beljaars et al. 1996; Findell and Eltahir 1997; Dirmeyer 1999; Koster et al. 2006) because of its significant role in controlling the partition of rainfall into infiltration and runoff and the partition of surface radiation energy into sensible and latent heat exchange with the atmosphere (Entekhabi

* Current affiliation: Department of Civil Engineering, Queen's School of Engineering, University of Bristol, Bristol, United Kingdom.

Corresponding author address: Rafael Rosolem, Department of Civil Engineering, Queen's School of Engineering, University of Bristol, 2.20 Queen's Building, University Walk, Bristol BS8 1TR, United Kingdom.
E-mail: rafael.rosolem@bristol.ac.uk

et al. 1996; Western and Blöschl 1999). The knowledge of soil water content is also important for vegetation dynamics and carbon cycle studies (Rodriguez-Iturbe and Porporato 2004; Cox et al. 2000; Zeng et al. 2008). However, despite its strong influence on the land surface–atmosphere interface, intermediate-scale soil moisture measurements useful for ecohydrometeorological applications have been difficult to obtain (Robinson et al. 2008) because the strong inherent heterogeneity of soil water content at small scales makes upscaling measurements to larger areas problematic (Blöschl 2001).

Recently, the assessment of soil moisture derived from measurements of cosmic-ray neutron intensity in air above the soil surface (Zreda et al. 2008) has emerged as a novel, noninvasive technique capable of providing area-averaged measurements of soil moisture at the horizontal scale of hectometers and the vertical scale of decimeters. Field tests of the cosmic-ray neutron method (also known as the ground albedo neutron sensing method) show that the integrated soil moisture derived from neutron intensity agrees well with area-averaged values obtained using distributed-sensor networks (Rivera Villarreyes et al. 2011; Franz et al. 2012b). The horizontal measurement area of a cosmic-ray probe (the radius within which 86% of the neutrons originate) is approximately 300–350 m and independent of soil moisture (Zreda et al. 2008, 2012; Desilets et al. 2010; Desilets 2011), while the depth of influence of the probe (similarly defined) varies between 76 cm in the dry soils and 12 cm in wet soils (Zreda et al. 2008, 2012).

Cosmic-ray neutron soil moisture probes are being deployed in the Cosmic-Ray Soil Moisture Observing System (COSMOS; Zreda et al. 2012), a network installed mainly within the continental United States with the objectives of providing soil moisture data to improve weather and climate predictions through assimilation of soil moisture into numerical models (Shuttleworth et al. 2013) and of providing validation to satellite remote sensing soil moisture data products, including those from the current Soil Moisture Ocean Salinity mission (SMOS; Kerr et al. 2001) and the future Soil Moisture Active Passive mission (SMAP; Entekhabi et al. 2010).

Primary cosmic rays (mainly protons) generate cascades of secondary high-energy neutrons through collisions with nuclei in the atmosphere (Hess et al. 1959). When these high-energy neutrons reach the soil, fast neutrons are created within the soil and near the surface. Some of the fast neutrons in the soil are scattered back to the near-surface atmosphere by diffusive processes to form a well-mixed, aboveground reservoir of neutrons whose density can be measured with the cosmic-ray probe. Hydrogen plays a crucial role because it has a much greater ability to stop (remove) neutrons than all

other elements present in soils combined. Because the amount of hydrogen is related to moisture content, the observed neutron intensity at neutron energies above a few electron volts (eV) is inversely correlated with soil-moisture (Zreda et al. 2008; Desilets et al. 2010). Nonetheless, it is important to recognize that cosmic-ray probes measure neutron intensity that responds to all forms of moisture present near the surface, including water present in the crystal lattice of minerals and ponded water (Franz et al. 2012a), snow (Desilets et al. 2010), organic matter (Franz et al. 2012a), vegetation (Hornbuckle et al. 2012; Franz et al. 2013b), and the atmosphere.

Because of its high variability in space and time (Wallace and Hobbs 1977; Dai 2006) and with an average residence time of approximately 8 days (Trenberth 1998), the influence of water vapor on fast neutron intensity needs to be appropriately allowed to provide a more reliable measure of neutron intensity that is directly associated with water present in the soil. Although early studies have attempted to identify the effect of water vapor on thermal (Bethe et al. 1940; Lockwood and Yingst 1956) and high-energy neutrons (Bercovitch and Robertson 1965; Chasson et al. 1966), no study has yet attempted to determine the fast neutron sensitivity to water vapor. In this paper we identify and evaluate the sensitivity of cosmic-ray probes to the hydrogen present as water vapor in the near-surface atmosphere.

The hypothesis we explore in this paper is that neutron intensity as measured by the cosmic-ray probes used in the COSMOS is affected by variations in the atmospheric water vapor that, when not corrected for, ultimately lead to bias in the derived soil moisture signal. To test this hypothesis, we employ a combination of neutron transport modeling and field measurements and observations. Based on modeling results, we propose a simple correction to cosmic-ray fast neutron data based on observed near-surface meteorological variables. The present study also supplements existing knowledge on the support volume for the probe by estimating the height of influence in the atmosphere.

2. Methods

a. Neutron transport modeling

Simulations of fast neutron flux were conducted using the Monte Carlo N-Particle eXtended (MCNPX) transport code, version 2.6 (Pelowitz 2007). In the model high-energy neutrons are generated on top of the atmosphere and then propagated down to land surface, where they produce fast neutrons. These fast neutrons are then moderated by the medium (soil or air), and equilibrium concentrations of neutrons are established throughout the domain. We count the number of

neutrons in the first layer of air above the soil surface (unless otherwise specified). The modeled horizontal domain comprised a $2\text{ km} \times 2\text{ km}$ grid. The vertical domain was defined as an approximate 8-km-high column above a 2-m-deep subsurface, with individual soil layers defined at 0, 2, 5, 10, 20, 40, 60, 80, 100, 150, and 200 cm below the ground and layers defined at 10-m intervals up to 1 km above the surface in the overlying atmosphere, with subsequent layers defined with coarser resolution. The soil is homogenous pure quartz sand (SiO_2) with a dry bulk density of 1.4 g cm^{-3} and porosity of 40% (i.e., a saturated water content of $0.40\text{ m}^3\text{ m}^{-3}$). The dry atmosphere is based on the U.S. Standard Atmosphere (COESA 1976), but for simplicity contains only N_2 and O_2 (78% and 22%, respectively). Each Monte Carlo simulation was performed with 500 000 incident particles, corresponding to an uncertainty of about $<1\%$ in the calculated average fast neutron flux with energy in the range 10–100 eV. The fast neutron flux is calculated relative to a reference simulation with dry atmosphere and dry soil.

b. Water vapor distribution in the atmosphere

We test the hypothesis that only variations in atmospheric water vapor within the first few hundred meters above the surface influence the count rate of cosmic-ray soil moisture probes. Therefore, simulated changes in atmospheric composition resulting from water vapor variations are applied only to the first kilometer above the surface. This gives an estimate of the atmospheric water vapor at height z (expressed as absolute humidity ρ_v , in kg m^{-3} , unless noted otherwise) based on near-surface air humidity measurements (Reitan 1963; Tomasi 1984; Tomasi and Paccagnella 1988; Parameswaran and Krishna Murthy 1990), thus,

$$\rho_v(z) = \rho_{v0} \exp\left[\frac{-(z - z_0)}{H}\right], \quad (1)$$

where ρ_{v0} (kg m^{-3}) is the absolute humidity at the surface, z_0 is the height above the ground (assumed to be zero), and H is the water vapor scale height, which is assumed to be $\sim 2.3\text{ km}$ based on Reitan's (1963) analysis of data from 15 stations in the United States and which is consistent with other studies (Tomasi 1977, 1978, 1984). Absolute humidity at the surface can be computed from meteorological measurements of temperature, barometric pressure, and atmospheric humidity (see the appendix). Assuming that humid air is a mixture of ideal gases, its density at any level can be calculated using, for instance, Eq. (3.6) in Brutsaert (1982). Once the absolute humidity at all levels, $\rho(z)$, is

available, the integrated water vapor (IWV) from the surface to a given level z in the atmosphere can be calculated from

$$\text{IWV}_{0-z} = \int_{z=0}^z \rho_v(z) dz, \quad (2)$$

where IWV (kg m^{-2}) corresponds numerically to the equivalent liquid water in millimeters were all water vapor to condense at the surface. In all model experiments, we allowed ρ_{v0} to vary between 0 and 23 g m^{-3} , consistent with the globally observed ranges (Dai 2006). Substituting Eq. (1) into Eq. (2) and assuming z_0 is defined at surface (i.e., $z_0 = 0$) gives an estimate of the value of IWV based only on surface meteorological variables (i.e., on ρ_{v0}); thus,

$$\text{IWV}_{0-z} = \rho_{v0} H \left[1 - \exp\left(\frac{-z}{H}\right)\right]. \quad (3)$$

Two numerical experiments are proposed to determine the height of influence in moist and dry atmospheric conditions. In these experiments, water vapor for the dry atmosphere was set to zero, while that in the moist atmosphere was specified by selecting an absolute humidity ρ_{v0} of 23 g m^{-3} at the surface and then calculating the equivalent profile to 1 km above ground at 10-m intervals using Eq. (1). In each sensitivity experiment, a series of MCNPX simulations were made and the fast neutron flux at the surface (normalized to a fully dry case with zero soil moisture and water vapor) was computed. In the first experiment, 10-m layers in the dry atmosphere were progressively replaced from the bottom (surface) to the top (1 km above ground) by moist layers. Thus, the first simulation was for a dry atmosphere. Then, in the second simulation, the dry atmosphere from the surface to 10 m was replaced by the equivalent moist atmosphere layer. In the third simulation, the dry atmosphere from the surface to 20 m was replaced by two moist atmosphere layers, and so on until the moist atmosphere reached 1 km and a fully moist atmosphere is simulated. The second sensitivity experiment was similar to the first, except that in this experiment, moist atmospheric layers were successively replaced by dry atmosphere layers, from the bottom, until the entire atmosphere was fully dry.

c. In situ measurements

In addition to model simulations, we carried out analyses using in situ measurements at two sites where meteorological data are available: Park Falls WLEF television tower in Wisconsin and the Santa Rita Experimental Range (SRER) in Arizona.

1) PARK FALLS WLEF TELEVISION TOWER

The 447-m tall WLEF television tower (Davis et al. 2003) is located near the northern edge of the Mississippi River basin, about 15 km east of Park Falls in northern Wisconsin (45.94598°N, 90.27238°W). The tower is located in the Chequamegon National Forest, and the surrounding area has elevation between 470 and 500 m and is mainly covered with deciduous broadleaf forest vegetation [International Geosphere–Biosphere Programme (IGBP) classification]. According to MacKay et al. (2002), the growing seasons are typically short and the winters are long and cold: mean temperatures in January and July are approximately -12° and 19° C, respectively.

The hourly meteorological measurements taken at different heights on the tower are used to develop the relationship between IWV and ρ_{v0} . Between 2006 and 2011 measurements of temperature and specific humidity are available at 30, 122, and 396 m above the ground and barometric pressure data are available at the lowest level. Data from the cosmic-ray soil moisture sensor (Model CRS-1000 from Hydroinnova LLC, Albuquerque, New Mexico, United States), installed about 1 m above the surface, are available from the COSMOS network (<http://cosmos.hwr.arizona.edu>) at hourly intervals from July until December 2011. When calculating IWV from Eq. (2), we interpolated temperature and specific humidity at 1-m intervals between the available measurement levels or extrapolated above or below the available measurement levels, as appropriate. We then calculated the pressure at each level from the ideal gas law following Eq. (3.13) in Shuttleworth (2012), as follows:

$$P(z) = P_{30m} \left[\frac{T(z)}{T_{30m}} \right]^{g/(R_d \Gamma_{\text{local}})}, \quad (4)$$

where $T(z)$ is the temperature at height z , g is the acceleration of gravity ($\sim 9.81 \text{ m s}^{-2}$), R_d is the gas constant for dry air ($\sim 287.1 \text{ J K}^{-1} \text{ kg}^{-1}$), and Γ_{local} is the local temperature lapse rate (K m^{-1}).

2) SANTA RITA EXPERIMENTAL RANGE

The site is located in the Sonoran Desert about 50 km south of Tucson in southeastern Arizona (31.9083°N, 110.8395°W) in the Santa Rita Experimental Range. Soil texture is characterized as sandy loam to at least 1-m depth and the site elevation is around 1000 m (Cavanaugh et al. 2011). Vegetation is dominated by creosote brush and covers approximately 24% of the area. Between 1971 and 2008, the mean annual temperature was 20° C and the mean annual precipitation 345 mm, distributed approximately evenly between

summer (monsoon rains) and winter (frontal rains). A cosmic-ray soil moisture sensor was installed at the site on June 2010 (approximately 1 m above the ground) as part of the COSMOS network. Further information about the site is available in Kurc and Benton (2010) and Cavanaugh et al. (2011).

In addition to meteorological and COSMOS instruments, the SRER site has a network of 180 time-domain transmission (TDT) probes distributed within the cosmic-ray probe footprint. These probes were installed June 2011 at 18 paired locations (at a total of 36 soil profiles) and at depths of 10, 20, 30, 50, and 70 cm. In January 2012, additional TDT probes were placed at 5-cm depth. The uncertainty in the TDT probes is estimated to be on the order of $0.02 \text{ m}^3 \text{ m}^{-3}$ (Franz et al. 2012b). Gravimetric soil samples were also collected within the cosmic-ray soil moisture footprint, following a similar sampling approach as used by the TDT network, for comparison with the cosmic-ray probe and TDT network estimates of area-averaged soil moisture. The period used in this analysis is from July 2011 to August 2012.

3. Results

a. Height of influence for a cosmic-ray soil moisture probe placed near ground

The reduction in neutron intensity at the surface when additional moist atmosphere layers are added to the background dry atmosphere is shown in Fig. 1. There is “noise” in this relationship as a result of the stochastic nature of the MCNPX simulations. To better identify the attenuation of neutron flux with height of perturbation, the light blue curve is fitted to the simulation points (corresponding to a sum of two exponential functions). The red line with circles corresponds to the increase of neutron flux computed at the surface as more layers from the background moist atmosphere are replaced by layers from the dry atmosphere. The fitted curve (again the sum of two exponential functions) is shown as an orange line.

Following the definition used in previous studies for the effective sensor depth (Zreda et al. 2008, 2012; Desilets et al. 2010; Desilets 2011; Franz et al. 2012a), the height of influence, defined here as the height of water vapor in the atmosphere that carries most of the influence on the modulation of incoming cosmic-ray neutrons, is computed as the height of perturbation at which there is a two e -folding difference (i.e., approximately an 86% change in sensitivity) in the neutron flux computed at the surface. This is accomplished by first scaling the individual flux values N to the zero to one range (i.e., $N - N_{\text{MIN}}$ divided by $N_{\text{MAX}} - N_{\text{MIN}}$, where

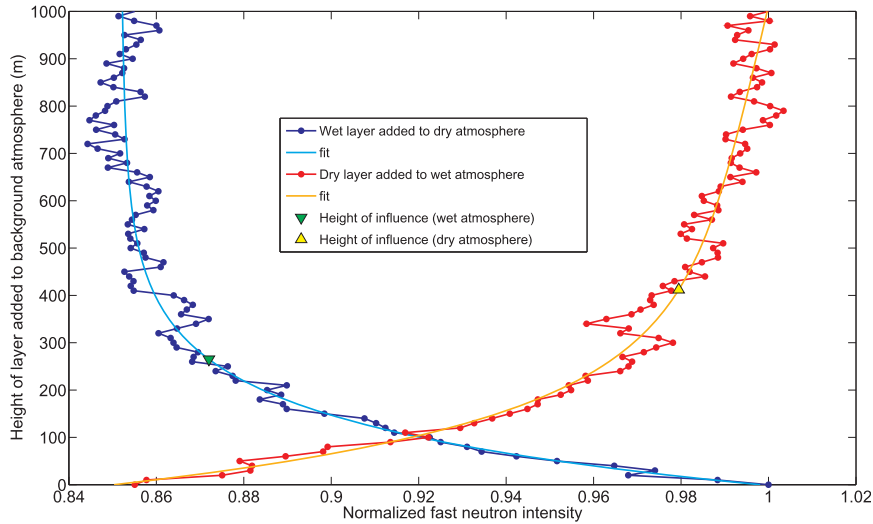


FIG. 1. Calculated height of influence for two sensitivity experiments. Model simulations are performed with a fully dry soil (i.e., $\theta = 0$); see section 3a for additional details. (Note that the absolute amount of water vapor at higher elevations is smaller than near the surface, so small fluctuations computed by the MCNPX model due to its stochastic nature tend to appear relatively greater at height.)

N_{MIN} and N_{MAX} are the minimum and maximum N values obtained with the fit, respectively). Notice that for the determination of the two e -folding distances, the maximum normalized value occurs at the bottom for the first sensitivity experiment (wet layers replacing background wet layers in the atmosphere), whereas for the second sensitivity experiment (dry layers replacing background dry layers in the atmosphere), this value is located at the top. On the basis of our simulations, the height of influence for a fully dry atmosphere is 412 m (yellow triangle), while the height of influence is 36% shorter (265 m) for a moist atmosphere (green triangle). For the evaluation of the effect of atmospheric water vapor on the neutron count signal of cosmic-ray probes, we therefore restrict consideration of the water vapor distribution in the atmosphere to the greater of these two heights of influence, that is, to within 412 m of the soil surface.

b. The effect of atmospheric water vapor on the cosmic-ray probe signal

We simulated 492 paired combinations of water vapor content (a total of 12 individual cases) and uniform soil moisture conditions (a total of 41 individual cases) using MCNPX in which soil moisture varied by $0.01 \text{ m}^3 \text{ m}^{-3}$ from fully dry (i.e., $\theta = 0$) to saturated soil, and the absolute humidity at the surface, ρ_{v0} , varied in intervals of 2 g m^{-3} from fully dry to 22 g m^{-3} (corresponding to IWV from 0 to 8.3 kg m^{-2} in the cosmic-ray probe footprint from the surface to 412 m). Figure 2a shows the

relationship between fast neutron flux and atmospheric water vapor for selected conditions of uniform soil moisture (θ) with atmospheric water vapor content (associated with ρ_{v0} and IWV). Changes in soil moisture clearly have the major influence on the modeled neutron flux signal and reduce the flux for a given value of water vapor content. The numerical simulations suggest that increased water vapor content within the 412-m atmospheric height of influence reduce the fast neutron count (Fig. 2a). The effect of water vapor on the fast neutron count can therefore be significant and should be considered.

To illustrate the effect of variations in atmospheric moisture on the atmospheric footprint, we analyze a simple case in the context of a hypothetical field measurement. Assume point A in Fig. 2a corresponds to a fast neutron intensity (with $N_{\text{CAL}} \approx 0.24$) measured on the day when the cosmic-ray probe was calibrated under a dry atmosphere, and on this day the soil moisture corresponds to $\theta = 0.20 \text{ m}^3 \text{ m}^{-3}$. At a later day, a new measurement of fast neutron ($N_{\text{MEAS}} = 0.21$) is made under moist conditions when $\rho_{v0} = 22 \text{ g m}^{-3}$ and $\text{IWV} = 6.9 \text{ kg m}^{-2}$. If changes in atmospheric conditions were neglected, the ensuing $\sim 12\%$ reduction in fast neutron flux would be associated with an increase in soil moisture from 0.20 to $0.30 \text{ m}^3 \text{ m}^{-3}$ (point B in Fig. 2a). However, point C in Fig. 2a shows that if the increased water vapor is taken into account, the $\sim 12\%$ reduction in the measured fast neutron intensity is solely due to changes in atmospheric conditions, and the true measured soil moisture remains unchanged.

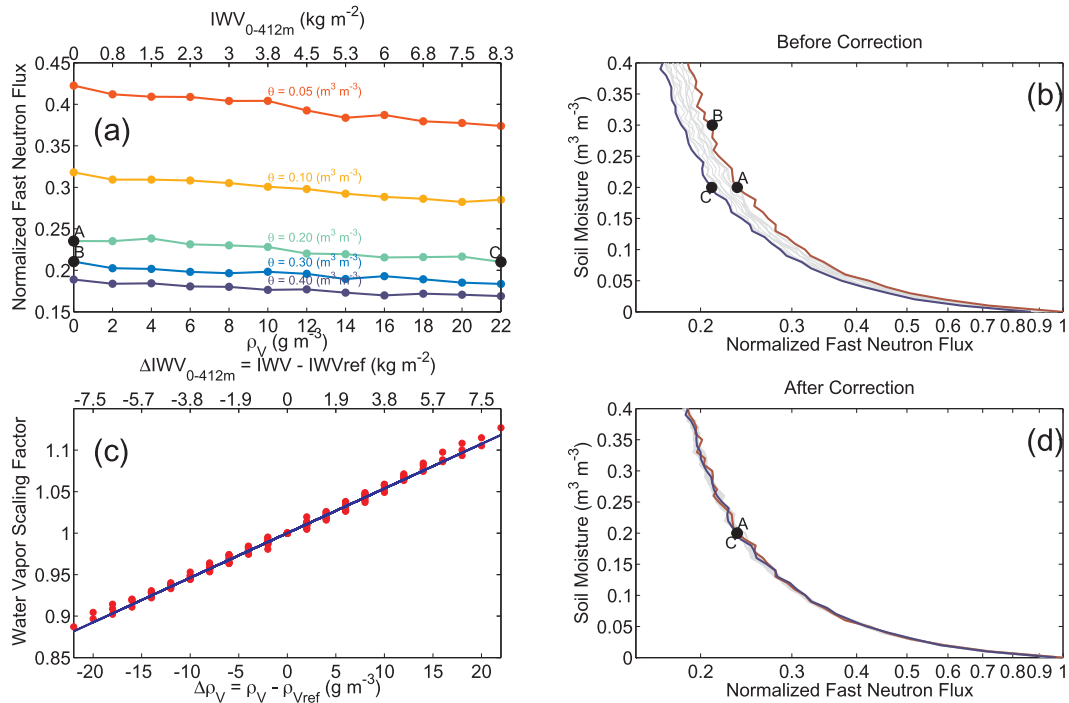


FIG. 2. (a) Response of normalized neutron flux to increasing atmospheric water vapor content for selected uniform soil moisture profiles (depicted in different colors). (b) The soil moisture–fast neutron relationship at the surface with different atmospheric water vapor contents (gray lines), with the driest case shown as a red curve and moistest case shown as a blue curve. Highlighted points A, B, and C are used to illustrate a hypothetical example of correction for the effect of water vapor. (c) The linear relationship (fitted with the blue line) between the water vapor scaling factor (C_{WV}) and the difference in atmospheric water vapor between the day when measurement is made and the day on which the cosmic-ray probe was calibrated. (d) Corrected form of the curves shown in (b) after water vapor correction has been applied with points A and C now overlapping each other. Note that the horizontal axes in (b) and (d) are defined in logarithmic scale. Refer to section 3b for additional details.

Figure 2b shows the relationship between soil moisture content and fast neutron intensity for a family of curves derived from different atmospheric water vapor conditions. The two highlighted curves correspond to the hypothetical case discussed in Fig. 2a, with points A, B, and C depicted. To account for changes in atmospheric conditions, the fast neutron intensity measured on a given day (N_{MEAS}) needs to be normalized to the atmospheric humidity on the day of calibration. In other words, the blue curve in Fig. 2b needs to be translated to lie on top of the red curve (the reference curve) so the observed neutron count at C is equivalent to the value at A. Because the correction takes the form of a translation of curves, only a single scaling factor (C_{WV}) is required:

$$N_{\text{CORR}} = N_{\text{MEAS}} C_{\text{WV}}, \quad (5)$$

with C_{WV} being a function of the difference between atmospheric water vapor observed on the day of measurement and conditions on the day of calibration. Using all 144 combinations of the curves shown in Figs. 2b and 2c, the relationship between the scaling factor C_{WV}

(unitless) and the two available measures of water vapor are as follows:

$$C_{\text{WV}} = 1 + 0.0054 \Delta \rho_{v0} \quad (R^2 = 0.99, \text{RMSE} = 0.00005), \quad (6)$$

$$C_{\text{WV}} = 1 + 0.0143 \Delta \text{IWV}_{0-412\text{m}} \quad (R^2 = 0.99, \text{RMSE} = 0.00005), \quad (7)$$

where $\Delta \rho_{v0} = (\rho_{v0} - \rho_{v0}^{\text{REF}})$, in units of g m^{-3} , and $\Delta \text{IWV}_{0-412\text{m}} = (\text{IWV}_{0-412\text{m}} - \text{IWV}_{0-412\text{m}}^{\text{REF}})$, in units of kg m^{-2} . [Note that Eqs. (6) and (7) can be formally related through Eqs. (1) and (3).] In the above equations, the superscript REF corresponds to reference values of the two quantities on the day of cosmic-ray probe calibration. The robustness of this correction factor is illustrated in Fig. 2d, which shows that the values originally shown in Fig. 2b are successfully translated to the reference curve (in this case, chosen to be the fully dry atmosphere case), and hence, points A and C are numerically identical.

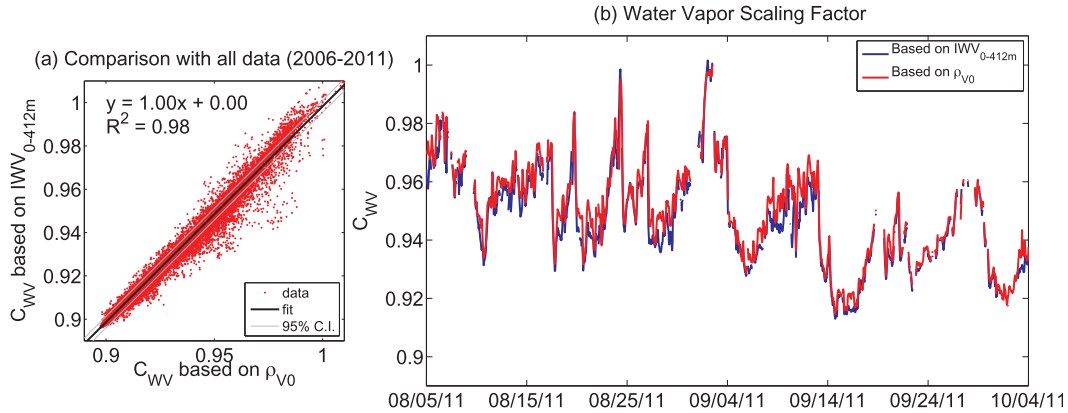


FIG. 3. At the Park Falls site, C_{WV} calculated based on ρ_{v0} and IWV in the cosmic-ray probe footprint, IWV_{0-412m} , shown (a) as a scatterplot for all available data between 2006 and 2011 and (b) as a sample time series.

It should be recognized that, although Eqs. (7) and (8) provide corrections that are necessary and beneficial when applied to the cosmic-ray soil moisture probes used in the COSMOS project, the modeling approach used to derive these equations necessarily involves simplifying assumptions. In the model used, the soil is assumed dry and horizontally homogeneous, the atmosphere is assumed to be well mixed, and atmospheric water is assumed present only in the form of water vapor, not some as fog, for example. The model integration used to derive the equations was restricted to 412 m (i.e., the estimate of height of influence made in section 3a for a totally dry atmosphere above a dry soil), and selecting this particular value is clearly also an assumption: selecting another value may have some effect on the values of the constants in Eqs. (7) and (8), although we believe this effect will be limited because the major influence is from atmospheric water, which is much closer to the surface than 412 m. Notwithstanding the simplifying modeling assumptions used in their derivation, we believe that the application of a correction for atmospheric changes using one of these two equations will lead to a significant and worthwhile improvement in the estimate of soil moisture derived from cosmic-ray probes, and in the next subsection we demonstrate use of the correction for atmospheric humidity using measurements at two COSMOS sites.

c. Comparing the performance of the proposed water vapor correction functions

If the profile of water vapor content within the probe footprint is available, then using Eq. (7) is the preferable correction procedure, but it will rarely be possible because it would involve using data from an atmospheric sounding. On the other hand, a correction based on surface moisture [Eq. (6)] is arguably less reliable but

requires only standard near-surface meteorological measurements and is therefore easier to apply.

We use the meteorological data from the WLEF tower at the Park Falls experimental site where ρ_{v0} and estimates of IWV_{0-412m} are both available in order to compare both of the proposed equations. Figure 3a shows that when both estimates are compared using available data from this site, the agreement is remarkably good in both daytime and nighttime conditions: linear correlations (not shown) give slopes of 1.01 and 0.98, intercepts of -0.01 and 0.01 , and R^2 of 0.99 and 0.98 for daytime and nighttime, respectively. The mean normalized bias [i.e., $[C_{WV}(\rho_{v0}) - C_{WV}(IWV_{0-412m})]$ normalized by $C_{WV}(IWV_{0-412m})$] is 0.16% for the entire period, with systematically higher uncertainty in the summer (0.22% for June–August) than winter (0.13% for December–February) and maximum normalized deviations 3.92% and 1.04% in the summer and winter, respectively. A comparison between the results that use the two estimates of C_{WV} for a 2-month period (August–October 2011) is shown in Fig. 3b.

Additional aspects of the application of water vapor corrections at Park Falls are illustrated in Fig. 4. The cosmic-ray sensor was installed and calibrated in late July under moist atmospheric conditions, corresponding to $IWV_{0-412m} = 7.4 \text{ kg m}^{-2}$ and $\rho_{v0} = 19.2 \text{ g m}^{-3}$, respectively. In consequence, the θ to N_{MEAS} relationship at this site is associated with high atmospheric humidity conditions, but the humidity decreases substantially toward much drier atmosphere in the winter (solid red line in Fig. 4a) compared to that when the sensor was calibrated (shown by the dashed black line). If changes in the water vapor content within the support volume are neglected, the neutron intensity suggests much higher count rates toward the end of 2011 (black line in Fig. 4b) relative to the count rates after water vapor correction (red line), implying the integrated soil moisture content

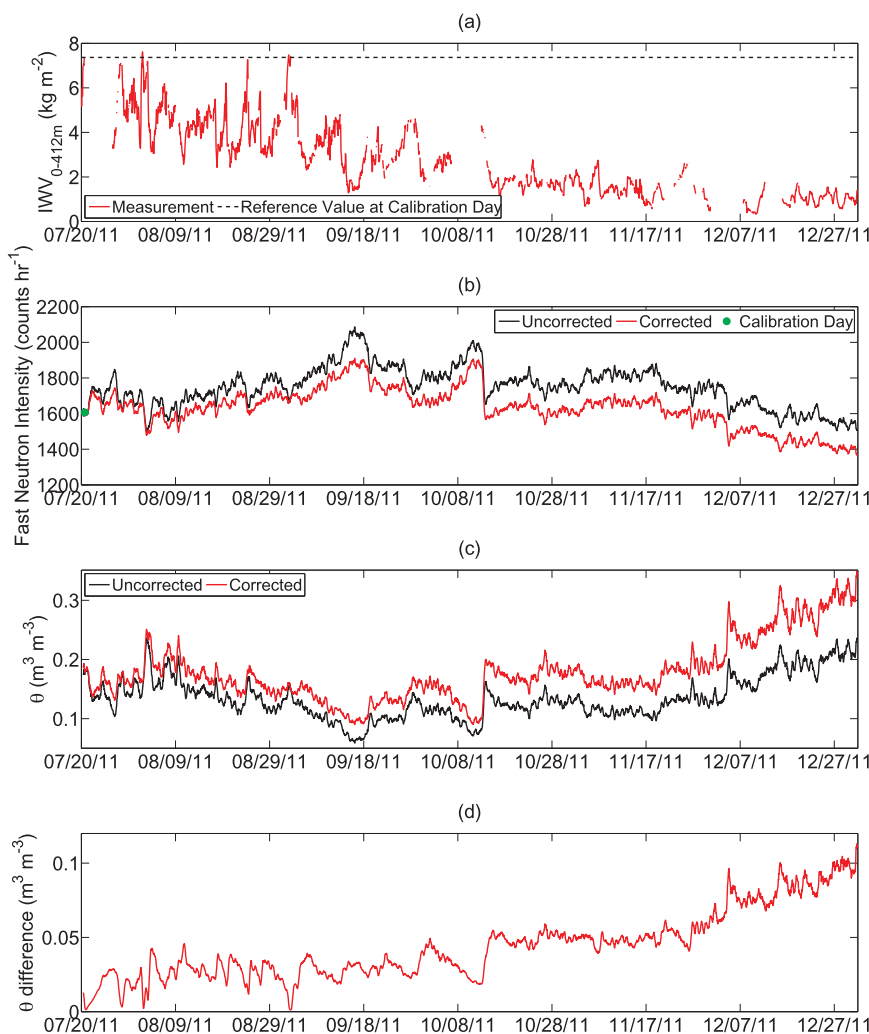


FIG. 4. Time series for the period of July–December 2011 at the Park Falls site of (a) IWV (kg m^{-2}) in the cosmic-ray probe footprint shown as red line, with the value on the day of calibration is shown as a dashed black line; (b) fast neutron intensity (counts per hour) before (black) and after (red) water vapor correction, with the fast neutron intensity on the day of calibration is shown as a green circle; (c) soil moisture ($\text{m}^3 \text{m}^{-3}$) before (black) and after (red) water vapor correction; and (d) difference between soil moisture before and after water vapor correction ($\text{m}^3 \text{m}^{-3}$). A 12-h running average has been applied to the fast neutron intensity and soil moisture observations.

is much lower than it actually was (Fig. 4c). As the atmosphere dries, the differences in soil moisture before and after correction is $0.11 \text{ m}^3 \text{m}^{-3}$ by December 2011 (Fig. 4d), corresponding to an increase in soil moisture from $0.24 \text{ m}^3 \text{m}^{-3}$ before to $0.35 \text{ m}^3 \text{m}^{-3}$ after. Note that for periods with missing data in Fig. 4a, the scaling factor C_{WV} was “gap filled” using the linear interpolation method: the use of alternative gap-filling methods (e.g., nearest neighbor) suggests that these give little discernible differences in the correction (not shown). The important point here is that it is important to seek to capture the seasonal variation in water vapor (even if some portions of the time series are estimated

using gap filling) in preference to disregarding the effect of variations in water vapor.

d. Demonstrating use of the water vapor correction function

We compare the time series of the cosmic-ray soil moisture probe with two other alternative measurements taken at the SRER site. The cosmic-ray probe was originally calibrated in January 2011 under extremely dry atmospheric conditions ($\rho_{\text{v}0} \approx 2.2 \text{ g m}^{-3}$) indicated by the dashed black line in Fig. 5a, but during the summer monsoons (2011 and 2012), the atmospheric humidity increases substantially ($\rho_{\text{v}0}$ approaches 20 g m^{-3}) before

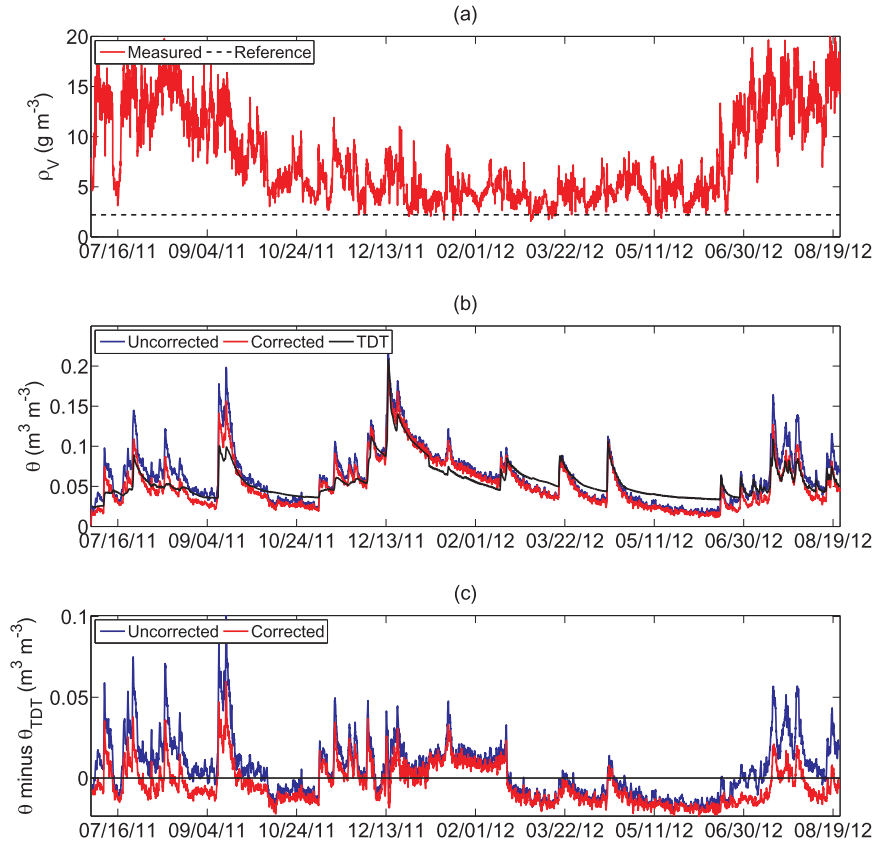


FIG. 5. Time series covering the period of July 2011 through August 2012 at the SRES site of (a) surface absolute humidity (ρ_v , g m^{-3}) shown as a red line, with the value on the day of calibration day is shown as a dashed black line; (b) soil moisture ($\text{m}^3 \text{m}^{-3}$) before (blue) and after (red) water vapor correction compared with the average soil moisture from the TDT network (black); and (c) the difference between soil moisture before (blue) and after (red) water vapor correction and the average soil moisture from the TDT network. A 12-h running average has been applied to the soil moisture observations.

falling again toward the end of the year, as indicated by the solid red line. If variations in atmospheric conditions are ignored (blue line in Fig. 5b), the higher humidity in summer (relative to when the probe was calibrated) means the resulting additional moderation of fast neutrons is incorrectly attributed to higher soil moisture. Accounting for changes in atmospheric water vapor yields estimates of the soil water content (red line) that better agree with the average soil moisture measured by the network of TDT sensors (black line). Additional sensors were installed at 5-cm depth on 1 January 2012, and the resulting improvement in the high frequency response of the average soil moisture can be seen by comparing the TDT-averaged observations during both summer periods.

An area-averaged soil moisture profile was derived from 180 TDT sensors installed (Franz et al. 2012b) in 18 paired profiles at 10, 20, 30, 50, and 70 cm within the footprint of the COSMOS probe (for further details,

see Franz et al. 2012b). Shallow soil layers have relatively higher contribution to the neutron signal (and hence, soil moisture estimated by the COSMOS probe) than deep layers; therefore, a depth-weighted soil moisture was calculated using the Cosmic-Ray Soil Moisture Interaction Code (COSMIC; for further details, see Shuttleworth et al. 2013). A comparison between the COSMOS-derived soil moisture and the depth-weighted value derived from the TDT network shows that the difference between these two sensing methods is reduced significantly, especially when the atmospheric conditions deviate largely from the reference atmosphere (i.e., in the summer period) (Figs. 5c and 6a,b). The systematic difference between COSMOS and the TDT observed during dry periods represents the inherent sensor-to-sensor uncertainty. This is consistent with reduced scatter in the soil moisture as measured by the cosmic-ray sensor relative to the average soil moisture measured by the TDT network (Figs. 6c,d).

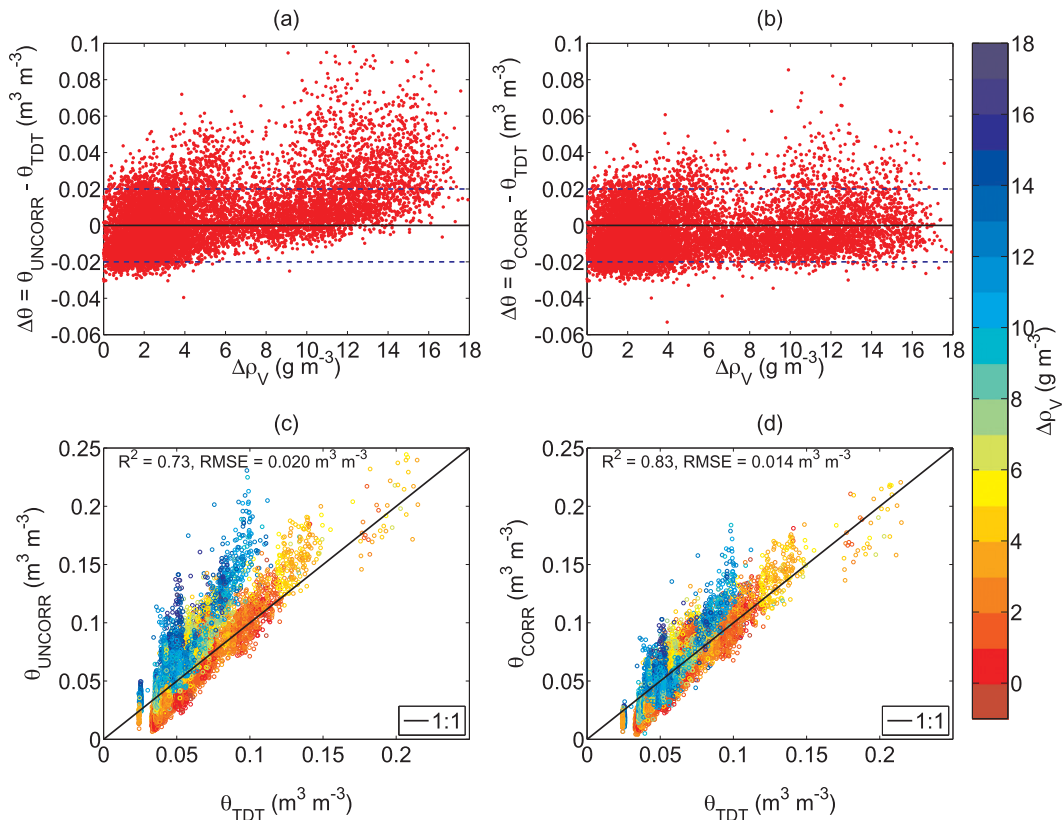


FIG. 6. Comparison between the difference of estimated soil moisture from the cosmic-ray sensor and the average from the TDT network ($\Delta\theta$) vs the deviation of absolute humidity from the reference value at the calibration day ($\Delta\rho_v$) (a) without and (b) with correction for atmospheric water vapor. The region within the dashed lines corresponds to the overall uncertainty in the TDT measurements (i.e., $\pm 0.02 \text{ m}^3 \text{m}^{-3}$). Estimated soil moisture ($\text{m}^3 \text{m}^{-3}$) at the SRES site given by the cosmic-ray probe vs the average soil moisture from the TDT network (c) without and (d) with correction for atmospheric water vapor. The color coding illustrates the deviation of atmospheric water vapor relative to that on the day when the cosmic-ray probe was calibrated.

On three specific dates, we also collected soil samples with a similar spatial distribution to that of the TDT network (i.e., for 18 soil moisture profiles). After applying the water vapor correction, the volumetric soil moisture estimated by the cosmic-ray soil moisture sensor agrees better with both the average soil moisture from the TDT network and the soil samples, as shown in Table 1.

4. Discussion and conclusions

On the basis of model simulations, we have derived a simple but important correction for the effect of variations of water vapor in the atmosphere on measurements made with cosmic-ray soil moisture sensors deployed in the COSMOS network. We have shown that if variations in atmospheric water vapor

TABLE 1. Comparison of area-averaged soil moisture obtained with three approaches on three distinct calibration days at SRER: 1) from cosmic-ray soil moisture probes before and after correction (θ_{UNCORR} and θ_{CORR} , respectively), 2) from a network of TDT sensors (θ_{TDT}), and 3) from soil samples (θ_{SAMPLE}). Both θ_{TDT} and θ_{SAMPLE} represent an average value from about 108 points (18 profiles with six depths) located within the approximate horizontal footprint estimated for the cosmic-ray sensor. As described in the text, the letters in brackets represent “codes” that allow us to identify which samples are considered statistically the same, based on Student’s t test at 5% significance level. For example, for 18 Dec 2011, θ_{CORR} , θ_{TDT} , and θ_{SAMPLE} can be considered significantly the same ([e] code), while θ_{UNCORR} cannot.

Soil moisture ($\text{m}^3 \text{m}^{-3}$)	11 Sep 2011	18 Dec 2011	18 Feb 2012
θ_{UNCORR}	0.151 ± 0.013 [a]	0.170 ± 0.013 [d]	0.090 ± 0.010 [f]
θ_{CORR}	0.122 ± 0.011 [b]	0.156 ± 0.013 [e]	0.083 ± 0.009 [g]
θ_{TDT}	0.092 ± 0.002 [c]	0.156 ± 0.014 [e]	0.079 ± 0.009 [g]
θ_{SAMPLE}	0.095 ± 0.031 [c]	0.154 ± 0.025 [e]	0.082 ± 0.018 [g]

TABLE 2. Parameters derived from linear fit of absolute humidity [$\rho_v(z)$] computed at three distinct heights ($z = 30, 122,$ and 396 m) and compared with actual measurements from the profile at the Park Falls site. The linear fit at a given height is given by $\rho_v^{\text{theor}}(z) = a \times \rho_v^{\text{obs}} + b$, where $\rho_v^{\text{theor}}(z)$ is calculated based on Eq. (1), while $\rho_v^{\text{obs}}(z)$ is measured at the site. Mean difference $\rho_v^{\text{theor}}(z) - \rho_v^{\text{obs}}(z)$ (in units of g m^{-3}) is also shown.

Height	Slope a	Intercept b	R^2	Mean difference (g m^{-3})
30 m	1.00	0.00	1.00	0.03 ± 0.14
122 m	1.01	0.08	0.98	0.12 ± 0.58
396 m	0.92	0.20	0.95	-0.19 ± 0.80

are not accounted for, especially those associated with strong seasonality, the neutron-derived soil moisture can be in error by as much as $0.10 \text{ m}^3 \text{ m}^{-3}$. The assumption adopted in our simulations, namely, an exponential decrease in water vapor [Eq. (1)] at heights near the surface, shows remarkably good comparison with observations at Park Falls (Table 2). The poorer (but still high) correlation further from the ground can be attributed to the lower quality of the measurements at height compared to those near the bottom of the tower (A. Desai 2012, personal communication).

Ideally, the water vapor scaling factor should be computed using observations of the water vapor profile from atmospheric sounding measurements using Eq. (7). However, because such observations are rare, an alternative correction, Eq. (6), which is based on near-surface meteorological measurements (see the appendix), is proposed. Both approaches yield results that are comparable and satisfactory. This means the correction can be easily implemented at sites where cosmic-ray probes are deployed, providing that standard near-surface meteorological observations are available. The maximum difference in C_{WV} between these two approaches was ~ 0.03 , which corresponds to only about 2% uncertainty in the corrected soil moisture. Our results suggest that this equivalence may be acceptable even under temperature inversion conditions when the stability of lower atmosphere layers limits the vertical transport of water vapor (Tomasi 1977). Arguably, this is because, for a few hundred meters above the surface, the atmosphere is still under the very strong influence of the ground. Much farther from the ground, at 3–5 km, observations (Tomasi and Paccagnella 1988; Parameswaran and Krishna Murthy 1990; Choudhury 1996) suggest that the simple exponential description we adopted for the water vapor profile may not be valid, but this is about 10 times higher than the adopted height of influence of the atmospheric water vapor on cosmic-ray measurements of soil moisture.

The comparison between the soil moisture derived from cosmic-ray sensors with the depth-weighted average from the network of TDT sensors at the SRER site shows that contamination of the sensor signal due to seasonal variations in water vapor can be successfully removed (e.g., Fig. 6). Since the water vapor signal is a relatively small correction to the soil moisture signal, it is important to consider inherent uncertainties in the meteorological measurements used to derive it. In other words, to consider whether measurement uncertainties in the meteorological observations compromise the correction and result in correction uncertainties similar to the difference between soil moisture before and after water vapor correction. A simple propagation of error analysis made using typical meteorological instrumentation uncertainty when measuring barometric pressure, air temperature, and relative humidity (i.e., $\delta P = 2 \text{ hPa}$, $\delta T = 0.5^\circ\text{C}$, $\delta \text{RH} = 3\%$, respectively) reveals that the degree of uncertainty in the computed soil moisture that results from meteorological sensor errors ($\sim 0.001 \text{ m}^3 \text{ m}^{-3}$) is on average approximately an order of magnitude less than the error that would be present were the water vapor correction not applied ($\sim 0.013 \text{ m}^3 \text{ m}^{-3}$).

It should be recognized, because the correction relates to changes of water vapor relative to a reference atmospheric condition (on the day of calibration), sites with strong seasonality are in most need of this correction (not the sites where atmospheric water vapor is greatest). In other words, a site located in the wet portion of the Amazon River basin (where atmospheric water vapor content is high) and another located in the Sahara desert (where atmospheric water vapor content is low) will both require similar small water vapor corrections given the lack of seasonality at both locations. On the other hand, for sites with strong seasonality in atmospheric water vapor, such as the SRER site, much larger corrections are needed.

Some example applications of the correction procedure at COSMOS probe sites were given in this paper, but unfortunately, only a few sites currently have the ancillary meteorological data readily available. However, as a result of this study, the new generation of cosmic-ray probes used in the COSMOS network will contain additional sensors recording external air temperature and relative humidity (surface pressure is already being measured by the probe) in order to allow real-time corrections for variations in atmospheric humidity. Current COSMOS sites will be retrofitted with the required meteorological sensors in order to standardize the COSMOS network database. Although this paper is focused on a correction for atmospheric moisture for probes used in the COSMOS, we encourage other networks that currently measure integrated soil

moisture via cosmic-ray sensors to adopt similar strategies to monitor and record variations in atmospheric water vapor in near-real time.

Acknowledgments. This study was supported by the Atmospheric Science, Hydrology, and Ecology programs of the U.S. National Science Foundation (Grant ATM-0838491). WLEF Park Falls tower observations were made possible with assistance from A. R. Desai and J. Thom of the University of Wisconsin–Madison, K. J. Davis of The Pennsylvania State University, D. Baumann of the U.S. Forest Service Northern Research Station, and J. Ayers of the Wisconsin Education Communications Board, with support from the National Science Foundation Biology Directorate Grant DEB-0845166. We also thank those who contributed in various ways to the quality of this study: Christopher Zweck (University of Arizona), Darin Desilets (Hydroinnova LLC), Gary Womack (Quaesta Corporation), Zulia Sanchez (University of Arizona), Ty Ferré (University of Arizona), James Broermann (University of Arizona), and the three anonymous reviewers for their valuable comments and suggestions.

APPENDIX

Computation of Absolute Humidity from Available Surface Meteorological Observations

Here we show the steps to compute absolute humidity (ρ_{v0}) from surface measurements of temperature (T_0), barometric pressure (P_0), and humidity (e.g., relative, specific, or water vapor mixing ratio). These are typical measurements available in automatic weather stations and eddy covariance flux towers. All quantities are in SI units unless otherwise noted. First, we calculate the water vapor pressure at saturation (e_{s0}) following the approach described by Bolton (1980):

$$e_{s0} = 6.112 \exp\left(\frac{17.67T_0}{243.5 + T_0}\right), \quad (\text{A1})$$

where the air temperature is given in degrees Celsius and e_{s0} is defined in hectopascals. Then, actual water vapor pressure (e_0) is calculated from the definition of relative humidity (RH_0 given in fractions):

$$e_0 = \text{RH}_0 e_{s0}. \quad (\text{A2})$$

Notice that if mixing ratio (w_0) observations are available instead of relative humidity, the water vapor pressure can be calculated using Eq. (2.61) in Wallace and Hobbs (1977):

$$e_0 = \frac{w_0}{w_0 + \varepsilon} P_0, \quad (\text{A3})$$

where $\varepsilon \approx 0.622$ is defined as the ratio of the molar mass of water vapor ($M_w \approx 18.02 \text{ g mol}^{-1}$) to the molar mass of dry air ($M_d \approx 28.96 \text{ g mol}^{-1}$; COESA 1976).

Absolute humidity (ρ_{v0}) can be calculated from the water vapor pressure (e_0) using the ideal gas law [Eq. (A4)]; alternatively, if specific humidity (q_0 , defined as the ratio of absolute humidity to air density, in kilograms of water vapor per kilograms of air) is available, it can be estimated by also making use of Dalton's law of partial pressures [Eq. (A5)]:

$$\rho_{v0} = \frac{e_0}{R_V T_0}, \quad (\text{A4})$$

$$\rho_{v0} = \frac{q_0}{1 - q_0} \left(\frac{P_0 - e_0}{R_d T_0} \right), \quad (\text{A5})$$

where $R_V = R^*/M_w \approx 461.5 \text{ J K}^{-1} \text{ kg}^{-1}$ is the gas constant for water vapor, $R_d = R^*/M_d \approx 287.1 \text{ J K}^{-1} \text{ kg}^{-1}$ is the gas constant for dry air, and $R^* \approx 8.314 \text{ J mol}^{-1} \text{ K}^{-1}$ is the universal gas constant. Depending on which humidity measurement is available, some steps can be skipped. Notice the absolute humidity calculated in Eqs. (A4) and (A5) is given in units of kg m^{-3} , and to be used in Eq. 7 it needs to be multiplied by 1000 (i.e., units given in g m^{-3}).

REFERENCES

- Beljaars, A. C. M., P. Viterbo, M. J. Miller, and A. K. Betts, 1996: The anomalous rainfall over the United States during July 1993: Sensitivity to land surface parameterization and soil moisture anomalies. *Mon. Wea. Rev.*, **124**, 362–383.
- Bercovitch, M., and B. C. Robertson, 1965: Meteorological factors affecting the counting rate of neutron monitors. *Proc. Ninth Int. Cosmic Ray Conf.*, London, United Kingdom, Institute of Physics and the Physical Society, 489–491.
- Bethe, H. A., S. A. Korff, and G. Placzek, 1940: On the interpretation of neutron measurements in cosmic radiation. *Phys. Rev.*, **57**, 573–587.
- Blöschl, G., 2001: Scaling in hydrology. *Hydrol. Processes*, **15**, 709–711, doi:10.1002/hyp.432.
- Bolton, D., 1980: The computation of equivalent potential temperature. *Mon. Wea. Rev.*, **108**, 1046–1053.
- Brutsaert, W., 1982: *Evaporation into the Atmosphere: Theory, History, and Applications*. Kluwer, 299 pp.
- Cavanaugh, M. L., S. A. Kurc, and R. L. Scott, 2011: Evapotranspiration partitioning in semiarid shrubland ecosystems: A two-site evaluation of soil moisture control on transpiration. *Ecohydrology*, **4**, 671–681, doi:10.1002/eco.157.
- Chasson, R. L., V. J. Kesselbach, and T. C. Sharma, 1966: Atmospheric water vapor and attenuation of the cosmic-ray nucleonic component. *J. Geophys. Res.*, **71**, 5183–5184.
- Choudhury, B. J., 1996: Comparison of two models relating precipitable water to surface humidity using globally distributed

- radiosonde data over land surfaces. *Int. J. Climatol.*, **16**, 663–675.
- COESA, 1976: *U.S. Standard Atmosphere, 1976*. NOAA, 227 pp.
- Cox, P. M., R. A. Betts, C. D. Jones, S. A. Spall, and I. J. Totterdell, 2000: Acceleration of global warming due to carbon-cycle feedbacks in a coupled climate model. *Nature*, **408**, 184–187.
- Dai, A., 2006: Recent climatology, variability, and trends in global surface humidity. *J. Climate*, **19**, 3589–3606.
- Davis, K. J., P. S. Bakwin, C. Yi, B. W. Berger, C. Zhao, R. M. Teclaw, and J. G. Isebrands, 2003: The annual cycle of CO₂ and H₂O exchange over a northern mixed forest as observed from a very tall tower. *Global Change Biol.*, **9**, 1278–1293.
- Desilets, D., 2011: Radius of influence for a cosmic-ray soil moisture probe: Theory and Monte Carlo simulations. Sandia Rep. SAND2011-1101, Sandia National Laboratories, Albuquerque, NM, 22 pp. [Available online at <http://prod.sandia.gov/techlib/access-control.cgi/2011/111101.pdf>.]
- , M. Zreda, and T. P. A. Ferre, 2010: Nature's neutron probe: Land surface hydrology at an elusive scale with cosmic rays. *Water Resour. Res.*, **46**, W11505, doi:10.1029/2009WR008726.
- Dirmeyer, P. A., 1999: Assessing GCM sensitivity to soil wetness using GSWP data. *J. Meteor. Soc. Japan*, **77**, 367–385.
- Entekhabi, D., I. Rodriguez-Iturbe, and F. Castelli, 1996: Mutual interaction of soil moisture state and atmospheric processes. *J. Hydrol.*, **184**, 3–17.
- , and Coauthors, 2010: The Soil Moisture Active Passive (SMAP) Mission. *Proc. IEEE*, **98**, 704–716.
- Findell, K. L., and E. A. Eltahir, 1997: An analysis of the soil moisture–rainfall feedback, based on direct observations from Illinois. *Water Resour. Res.*, **33**, 725–735.
- Franz, T. E., M. Zreda, T. P. A. Ferre, R. Rosolem, C. Zweck, S. Stillman, X. Zeng, and W. J. Shuttleworth, 2012a: Measurement depth of the cosmic ray soil moisture probe affected by hydrogen from various sources. *Water Resour. Res.*, **48**, W08515, doi:10.1029/2012WR011871.
- , —, R. Rosolem, and T. P. A. Ferre, 2012b: Field validation of cosmic-ray soil moisture probe using a distributed sensor network. *Vadose Zone J.*, **11**, vjz2012.0046, doi:10.2136/vjz2012.0046.
- , —, and —, 2013a: A universal calibration function for determination of soil moisture with cosmic-ray neutrons. *Hydrol. Earth Syst. Sci.*, **17**, 453–460, doi:10.5194/hess-17-453-2013.
- , and Coauthors, 2013b: Ecosystem scale measurements of biomass water using cosmic-ray neutrons. *Geophys. Res. Lett.*, doi:10.1002/grl.50791, in press.
- Hess, W. N., H. W. Patterson, and R. Wallace, 1959: Cosmic-ray neutron energy spectrum. *Phys. Rev.*, **116**, 445–457.
- Hornbuckle, B., S. Irvin, T. Franz, R. Rosolem, and C. Zweck, 2012: The potential of the COSMOS network to be a source of new soil moisture information for SMOS and SMAP. *Proc. 2012 IEEE Int. Geoscience and Remote Sensing Symp.*, Munich, Germany, IEEE, 1243–1246.
- Kerr, Y. H., P. Waldteufel, J.-P. Wigneron, J. Martinuzzi, J. Font, and M. Berger, 2001: Soil moisture retrieval from space: The Soil Moisture and Ocean Salinity (SMOS) mission. *IEEE Trans. Geosci. Remote Sens.*, **39**, 1729–1735.
- Koster, R. D., and Coauthors, 2006: GLACE: The Global Land–Atmosphere Coupling Experiment. Part I: Overview. *J. Hydrometeorol.*, **7**, 590–610.
- Kurc, S. A., and L. M. Benton, 2010: Digital image-derived greenness links deep soil moisture to carbon uptake in a creosote bush-dominated shrubland. *J. Arid Environ.*, **4**, 585–594.
- Lockwood, J. A., and H. E. Yingt, 1956: Correlation of meteorological parameters with cosmic-ray neutron intensities. *Phys. Rev.*, **104**, 1718–1722.
- MacKay, D. S., D. E. Ahl, B. E. Ewers, S. T. Gower, S. N. Burrows, S. Samanta, and K. J. Davis, 2002: Effects of aggregated classifications of forest composition on estimates of evapotranspiration in a northern Wisconsin forest. *Global Change Biol.*, **8**, 1253–1265.
- Parameswaran, K., and B. V. Krishna Murthy, 1990: Altitude profiles of tropospheric water vapor at low latitudes. *J. Appl. Meteor.*, **29**, 665–679.
- Pelowitz, D. B., 2007: MCNPX user's manual, version 2.6.0. Los Alamos National Laboratory Rep. LA-CP-07-1473.
- Reitan, C. H., 1963: Surface dew point and water vapor aloft. *J. Appl. Meteor.*, **2**, 776–779.
- Rivera Villarreyes, C. A. R., G. Baroni, and S. E. Oswald, 2011: Integral quantification of seasonal soil moisture changes in farmland by cosmic-ray neutrons. *Hydrol. Earth Syst. Sci.*, **15**, 3843–3859, doi:10.5194/hess-15-3843-2011.
- Robinson, D. A., and Coauthors, 2008: Soil moisture measurement for ecological and hydrological watershed-scale observatories: A review. *Vadose Zone J.*, **7**, 358–389, doi:10.2136/vzj2007.0143.
- Rodriguez-Iturbe, I., and A. Porporato, 2004: *Ecology of Water-Controlled Ecosystems: Soil Moisture and Plant Dynamics*. Cambridge University Press, 460 pp.
- Shuttleworth, W. J., 2012: *Terrestrial Hydrometeorology*. John Wiley & Sons, 448 pp.
- , R. Rosolem, M. Zreda, and T. Franz, 2013: The Cosmic-Ray Soil Moisture Interaction Code (COSMIC) for use in data assimilation. *Hydrol. Earth Syst. Sci. Discuss.*, **10**, 1097–1125, doi:10.5194/hessd-10-1097-2013.
- Tomasi, C., 1977: Precipitable water vapor in atmospheres characterized by temperature inversions. *J. Appl. Meteor.*, **16**, 237–243.
- , 1978: On the water vapour absorption in the 8–13 μm spectral region for different atmospheric conditions. *Pure Appl. Geophys.*, **116**, 1063–1076.
- , 1984: Vertical distribution features of atmospheric water vapor in the Mediterranean, Red Sea and Indian Ocean. *J. Geophys. Res.*, **89**, 2563–2566.
- , and T. Paccagnella, 1988: Vertical distribution features of atmospheric water vapour in the Po Valley area. *Pure Appl. Geophys.*, **127**, 93–115.
- Trenberth, K. E., 1998: Atmospheric moisture residence times and cycling: Implications for rainfall rates and climate change. *Climatic Change*, **39**, 667–694.
- Wallace, J. M., and P. V. Hobbs, 1977: *Atmospheric Science: An Introductory Survey*. Academic Press, 467 pp.
- Western, A. W., and G. Blöschl, 1999: On the spatial scaling of soil moisture. *J. Hydrol.*, **217**, 203–224.
- Zeng, X. D., X. B. Zeng, and M. Barlage, 2008: Growing temperate shrubs over arid and semiarid regions in the Community Land Model–Dynamic Global Vegetation Model. *Global Biogeochem. Cycles*, **22**, GB3003, doi:10.1029/2007GB003014.
- Zreda, M., D. Desilets, T. P. A. Ferré, and R. Scott, 2008: Measuring soil moisture content non-invasively at intermediate spatial scale using cosmic-ray neutrons. *Geophys. Res. Lett.*, **35**, L21402, doi:10.1029/2008GL035655.
- , W. J. Shuttleworth, X. Zeng, C. Zweck, D. Desilets, T. Franz, R. Rosolem, and T. P. A. Ferre, 2012: COSMOS: The Cosmic-Ray Soil Moisture Observing System. *Hydrol. Earth Syst. Sci. Discuss.*, **9**, 4505–4551, doi:10.5194/hessd-9-4505-2012.